Articles in Press, J. Med. Biol. Eng. (February 14, 2012), doi: 10.5405/jmbe.923

Title: An Automated Classification Method for Single Sweep Local Field Potentials Recorded from Rat Barrel Cortex under Mechanical Whisker Stimulation

Author list: Mufti Mahmud[1,4], Davide Travalin[2], Alessandra Bertoldo[3], Stefano Girardi[1], Marta Maschietto[1], Stefano Vassanelli[1,*]

Affiliation of authors:

[1]NeuroChip Laboratory, Dept. of Human Anatomy & Physiology, University of Padova, 35131 Padova, Italy

[2]During the work author was with: Dept. of Information Engineering, University of Padova, 35131 Padova, Italy. Now: Clinical Department, St. Jude Medical Italia S.p.A, 20864 Agrate Brianza, Italy

[3]Dept. of Information Engineering, University of Padova, 35131 Padova, Italy

[4]Institute of Information Technology, Jahangirnagar University, Savar, 1342 Dhaka, Bangladesh

Running title: **Automated Classification of Single Sweep Local Field Potentials**

*Corresponding author: Stefano Vassanelli

Tel: +39 049 8275337

Fax: +39 049 8275301

E–mail: stefano.vassanelli@unipd.it

ABSTRACT

Understanding brain signals as an outcome of brain's information processing is a challenge for the neuroscience and neuroengineering community. Rodents sense and explore the environment through whisking. The local field potentials (LFPs) recorded from the barrel columns of the rat somatosensory cortex (S1) during whisking provide information about the tactile information processing pathway. Particularly when using large-scale high-resolution neuronal probes, during each experiment many single LFPs are recorded as an outcome of underlying neuronal network activation and averaged to extract information. However, single LFP signals are frequently very different from each other and extracting information provided by their shape is a useful way to better decode information transmitted by the network. In this work, we propose an automated method capable of classifying these signals based on their shapes. We used template matching approach to recognize single LFPs and extracted the contour information from the recognized signal to generate a feature matrix, which is then classified using the intelligent K–means clustering. As an application example, shape specific information (e.g., latency, and amplitude) of LFPs evoked in the rat somatosensory barrel cortex and used in decoding the rat whiskers information processing pathway is provided by the method.

Keywords: Local field potentials, Barrel cortex, Whisker stimulation, LFP classification, Neuronal signal analysis

1. Introduction

During the last decade many researchers took their interest in deciphering brain activity as an outcome of the activation of underlying neuronal networks. To do so, they have developed high resolution neuronal probes capable of providing unprecedented information about neuronal circuits [1]. These recording tools deliver huge amount of recordings containing spiking activity as well as field potentials generated in the brain area under investigation. To understand the signal propagation among different cortical layers and the information processing pathways, scientists have relied on the local field potentials (LFPs). Due to the fact that the scientists use stimulus–locked field potentials to assess and understand the effect of stimuli on a brain area(s), the LFPs provide a 'fingerprint' of the stimuli's effect on activity propagation in neuronal networks of the brain region under study [2]. The conventional way of analyzing these LFPs is to record for a period of time and then obtain a stimulus–locked average. However, experimental studies have shown that the individual information provided by a single sweep may disappear if one considers an average over several runs under the same stimulus conditions [3]. Furthermore, to understand certain issues of the brain (for example, signal processing pathway and cortical layer activation order [8]) and for certain operations (for example, current source density analysis) signal shape plays an important role [4]. It is thus implied that different shapes in the single sweep signals denote different neuronal network activity. Therefore, a shape based classification method is required to extract different LFP shapes present in a pool of single LFPs to decipher the neuronal network activity from the LFPs. A wide range of research has been conducted in detection and sorting of neuronal spikes [5], but till date there is no method capable of performing similar sorting for the single LFPs.

In this work, we present a method for single LFPs classification based on the shape of the signals. This method exploits information about the signal contour to perform the classification. The terms classification, signal sorting and clustering will be used synonymously throughout the text.

As the method uses the shape information of the LFPs for the classification, it is worth taking a look to the contour characteristics of the signals. The LFPs recorded from a barrel column of the rat S1 cortex by stimulating the corresponding whisker can be differentiated by their specific characteristics based on the depth or layer they are recorded from, thanks to the existing research on the rat barrel cortex. Figure 1 shows a depth profile during one of our experiments. The signals were recorded equidistantly at 90 μm pitch from the cortical surface to deep cortical layer, but only representative signals from each layer are shown.

As illustrated by Ahrens and Kleinfeld [6] and Kublik [7], the cortical LFPs can be characterized by four consecutive events. Event 1 (E1): a small positive / negative peak; event 2 (E2): a dominant negative peak; event 3 (E3): a slow positive peak; and event 4 (E4): a slow negative peak. Usually in upper cortical layers (I, II) the signals are expected to have positive E1 followed by the E2, E3 and E4. In the signals recorded from the middle layers (III, IV, and V) the E1 is absent and they are expected to have the E2, followed by the E3 and E4. In deeper brain cortex (layer VI), the E2 becomes smaller and usually gets divided into two smaller negative peaks (negative E1, and E2), followed by E3 and E4 [8]. These characteristics of the signals and with the a priori information about the recording position are used in generation of the template.

The single signal sorting is done in four steps: (1) smoothing of single LFPs within individual recording sweeps; (2) template generation; (3) single LFP recognition through

template matching and (4) clustering of recognized single signals. The smoothing is performed using nonlinear least square estimation to remove the spatial oscillations and noise in the single LFPs. Once the signals are estimated, for each signal the starting and end of the response is determined as the stimulus–onset and end of signal, respectively. An average of the response part is considered as a template to be used for signal recognition. This method matches the contour of the template for recognition of the single signals which is compared to each of the single LFP's contour with a predefined boundary condition. If the single LFP falls within the boundary condition, the single signal is considered to be recognized. Once the single LFP recognition is over, intelligent K–means clustering is applied on the recognized LFPs to classify them according to their shapes. The classified or clustered single LFPs are then locally averaged. In agreement with previously reported results [9] averaged local LFPs show different shape and amplitude characterizing those signals. These parameters provide insights about underlying neuronal network activity and on the whiskers signal processing pathways. However, clustered averages of the single LFPs revealed differences in event latencies and amplitudes, thus demonstrating differentiated network activity within the same cortical area at different times but after the same stimulus.

2. Materials and Methods

I. Clustering Method

A. Template Generation

The first step of the template generation is smoothing. As the single LFPs contain spontaneous neural oscillations and noise, it is often difficult to have precise information about the individual signal events. Thus, removal of oscillations and noise is required. In case of spike

signals detection it would be possible to use a high pass filter to get rid of slow oscillations, but as our signals contain mainly LFPs (in the range of 1 to 100 Hz) using a simple filter will distort the response. Therefore, we removed oscillations and noise through smoothing / estimation using the Gauss–Newton based nonlinear least square method.

To estimate the single sweep signals we considered a generalized measurement error based model (eq. 1).

$$x_k = y_k + v_k$$

$$\Rightarrow x_k = g(t_k, \boldsymbol{x}^*) + v_k \quad (1)$$

where the model parameter, $\boldsymbol{x}^* = [x^*_1, x^*_2, \ldots, x^*_M]^T$ is a vector and t is the time, with $k=1,\ldots,N$ and N being the total data points present in a single sweep signal. As per this model, the recorded signal at time t_k is an integrated sum of the model's response (y_k) and the measurement error (v_k), under the assumption that the measurement error is additive, zero mean and Gaussian in distribution. It is further assumed that time is the only independent variable and the measurements are done precisely at known times, t_k.

The estimation parameter vector is calculated based on the minimization of the prediction error, $e(\boldsymbol{x}^*)$. When the true value of $\boldsymbol{x}^*$ is unknown, a generic value of $\boldsymbol{x}^*$ is used that minimizes the difference between the data vector and the model prediction for that particular value of $\boldsymbol{x}^*$, i.e., $e(\boldsymbol{x}^*) = \boldsymbol{x} - g(t, \boldsymbol{x}^*)$. The optimal $\boldsymbol{x}^*$ value is chosen iteratively based on the smallest possible value of $e(\boldsymbol{x}^*)$. The goodness of the chosen $\boldsymbol{x}^*$ value is thus given by the Euclidean norm of a generic vector $R = [r_1, \ldots, r_N]^T$ and is given by:

$$\|R\|^2 = \boldsymbol{r}^T\boldsymbol{r} = \sum_{i=1}^{N} r_i^2$$

And the weighted Euclidean norm is given by:

$$\|R\|_{\Phi}^2 = \boldsymbol{r}^T\boldsymbol{\Phi}\boldsymbol{r} = \sum_{i=1}^{N} \frac{r_i^2}{\Phi_i}$$

where Φ is defined as a positive square matrix of $N \times N$ dimension.

If the above formalism of parameter estimation fails to provide satisfactory smoothing, a non–linear least square method is used, which is more effective, but computationally expensive. This validation is done through detection of the prestimulus part of a signal and comparing the standard deviation before and after smoothing. It has been empirically found that if the difference of standard deviations between pre- and post-smoothing is more than half of the standard deviation of the original signal, a more sophisticated smoothing technique is required.

From the definition of least square [10], for a given vector function $f(x)$: $\mathbb{R}^n \mapsto \mathbb{R}^m$ with $m \geq n$, we want to minimize the norm of the function $\|f(x)\|$ or equivalently find:

$$x^* = argmin_x\{F(x)\} \quad (2)$$

Where x^* is a local minimizer for $F(x)$ meaning that for a set of arguments x^*, the $F(x)$ is kept minimal within a range δ, with δ being a small positive number.

$$F(x) = \frac{1}{2}\sum_{i=1}^{m}\left(f_i(x)\right)^2 = \frac{1}{2}\|f(x)\|^2 = \frac{1}{2}f(x)^T f(x) \quad (3)$$

Now adding a weight function (the covariance matrix of the prediction error, Σ_v) to eq. 3 and rewriting the model of eq. 1 to eq. 4 to calculate the prediction error, an analytical solution of the problem (in eq. 5) can be obtained.

$$x = y(x^*) + v \tag{4}$$

$$x^* = (y^T \Sigma_v^{-1} y)^{-1} y^T \Sigma_v^{-1} x \tag{5}$$

where *y* is the model prediction with *x** set of parameters and *x* is the actual measured values.

To solve the nonlinearity, the initial value at $x_k^*, k = 0$ is assigned to the parameter vector. Then, the model is linearized around the initial value using the first order Taylor's expansion. Thus the problem can be represented by eq. 6.

$$\Delta x = P \Delta x^* + v \tag{6}$$

where *P* is a partial derivative matrix of $N \times M$ size with predicted values using the initial condition ($x_k^*, k = 0$).

Now, the linear formula can be used to estimate the parameters as in eq. 7 and a new parameter vector is obtained by eq. 8. This iterative process is repeated until the cost function stabilizes or falls below a threshold.

$$\Delta x^* = (P^T \Sigma_v^{-1} P)^{-1} P^T \Sigma_v^{-1} x \tag{7}$$

$$x_{k+1}^* = x_k^* + \Delta x_k^* \tag{8}$$

166 The estimated signals are scanned for occurrence of the aforementioned events. In usual
167 cases, the stimulus–onset defines the starting point and the end of response defines the end of the
168 template. As all the signals don't have the same end of response, signals are zero–padded and
169 averaged to obtain a template.

170 *B. Single Sweep Recognition*

171 Once the template is generated, the contour of the template is used to recognize the single
172 signals. Boundary conditions (lower and upper bounds) are imposed to facilitate the recognition
173 process and for calculating the boundary conditions.

174 $$V_{tmp} = \frac{1}{N}\sum_{i=1}^{N}[Sw_i(k) - Temp(k)]^2 \quad (9)$$

175 where *Sw* is the zero–padded and truncated single LFPs and *Temp* is the template.

176 The upper and lower bounds are calculated using eq. 10 and eq. 11.

177 $$Up(k) = Temp(k) + (a * \left(V_{tmp}(k)\right)^{1/2} + b) \quad (10)$$

178 $$Low(k) = Temp(k) - (a * \left(V_{tmp}(k)\right)^{1/2} + b) \quad (11)$$

179 where *a, b* are constant; the values of *a, b* (*a = STD(Temp),* and *b = 3*STD(Temp)*) are
180 determined empirically and *STD* standing for standard deviation.

181 A signal is considered as recognized (following the contour of the template), if and only
182 if all of its data points lie within the range of the boundary conditions.

183 *C. Clustering the Recognized LFPs*

Once the single LFP signals are recognized, they are individually scanned for events (E1–E4) that characterize the LFPs. For this event detection purpose we used an *in–house* algorithm [8]. These shape characterizing events of the signal recorded from a particular cortical position are used to form the feature matrix to be clustered. For our clustering algorithm we used a feature matrix of size $200 \times N$, i.e., from each single sweep we extracted 200 points related to the events. However, as the shape information is important for the clustering, these 200 points were not selected as evenly distributed among the whole signal; rather more points were selected around the events to represent the signal shape characteristics at a higher resolution.

For our purpose of clustering we used the 'intelligent K–means method' of classifying the feature matrix generated from the recognized LFPs, which is an updated version of the classical K–means method [11–12].

The K–means method usually is applied to a dataset involving a set of N entities, I, a set of M features, V, and an entity–to–feature matrix $Y=(y_{iv})$, where y_{iv} is the value of feature $v \in V$ at entity $i \in I$. The method produces a partition $S=\{S_1, S_2, \ldots, S_K\}$ of I in K non–overlapping classes S_k, referred to as clusters, each with a centroid $c_k=(c_{kv})$, an M–dimensional vector in the feature space ($k=1,2,\ldots K$). Centroids form set $C=\{c_1, c_2, \ldots, c_K\}$. The criterion, minimized by the method, is the within–cluster summary distance to centroids:

$$W(S,C) = \sum_{k=1}^{K} \sum_{i \in S_k} d(i, c_k) \qquad (12)$$

where d is the squared Euclidean distance.

Given K M–dimensional vectors c_k as cluster centroids, the algorithm updates clusters S_k according to the Minimum distance rule: for each entity i in the data table, its distances to all

centroids are calculated and the entity is assigned to its nearest centroid. Given the clusters S_k, centroids c_k are updated according to the distance d in eq. 12, $k=1, 2,..., K$. Specifically, c_k is calculated as the vector of within–cluster averages as d in eq. 12 is the squared Euclidean distance. This process is reiterated until clusters S_k stabilize.

However, this approach has as a severe drawback that the cluster number, K, is required to be supplied before start of the classification. To overcome this, we adapted the intelligent K–Means (*i*K–Means) clustering method as proposed in [13]. This *i*KMeans method uses an anomalous pattern (AP) to find out the appropriate number of clusters.

The AP algorithm starts from an entity, which is the farthest from the origin, as the initial centroid c. After that, a one–cluster version of the generic K–Means is used. The current AP cluster S is defined as the set of all those entities that are closer to c than to the origin, and the next centroid c is defined as the center of gravity of S. This process is iterated until convergence.

Finally, when the single LFPs are classified into their respective clusters, they are cluster–wise averaged for further processing.

II. Neurosurgery and Signal Acquisition

A. Animal Preparation

All procedures followed Italian Ministry of Health Guidelines and were approved by the Eithical Committee of the University of Padova, Italy. P30–P40 male rats were anesthetized with an induction mixture of Tiletamine (2 mg/100 g weight) and Xylazine (1.4 g/100 g weight). The anesthesia level was monitored throughout the experiment by testing eye and hind–limb reflexes, respiration and checking the absence of whiskers' spontaneous movements. Whenever necessary,

additional doses of Tiletamine (0.5 mg/100 g weight) and Xylazine (0.5 g/100 g weight) were provided.

During the surgery and the recording section, animals were kept on a common stereotaxic apparatus under a stereomicroscope and fixed by teeth– and ear–bars. The body temperature was constantly monitored with a rectal probe and maintained at about 37℃ using a homeothermic heating pad. Heart beat was assessed by standard ECG. To expose the cortical area of interest, anterior–posterior opening in the skin was made along the medial line of the head, starting from the imaginary eyeline and ending at the neck. While the skin was kept apart using halsted–mosquito hemostats forceps, the connective tissue between skin and skull was gently removed by means of a bone scraper. Thus, the skull over the right hemisphere was drilled to open a window in correspondence of the S1 cortex (–1 ÷ –4 AP, +4 ÷ +8 ML) [14]. Meninges were then carefully cut by means of forceps at coordinates –2.5 AP, +6 LM for the subsequent insertion of the recording micropipette.

Throughout experiment, the brain was bathed by a standard Kreb's solution (in mM: NaCl 120, KCl 1.99, $NaHCO_3$ 25.56, KH_2PO_4 136.09, $CaCl_2$ 2, $MgSO_4$ 1.2, glucose 11), constantly oxygenated and warmed at 37° C. At the end of the surgery, contralateral whiskers were trimmed at about 10 mm from the mystacial pad.

B. Whiskers Stimulation and Recording

The recording of LFPs from S1 was performed by means of borosilicate micropipettes (1 MΩ resistance), filled with Kreb's solution. The pipette was fixed to a micromanipulator at 45°–tilted respect to the vertical axis of the manipulator, thus being inserted perpendicularly to S1

cortex surface. Figure 2 outlines the various parts of the signal acquisition setup during our experiment.

LFPs were evoked by single whiskers mechanical stimulation performed with a custom–made speaker that provides dorsal–ventral movements through a connected tube. The speaker was driven by a waveform generator (Agilent 33250A 80 MHz, Agilent Technologies) providing 1 ms, 10 V square stimuli with 150 ms delay. Each whisker, starting from the posterior group, was individually inserted into the tube and the corresponding response was checked at –750 μm depth (cortical layer IV), in order to find the most responsive whisker for the selected recording point in the cortex. The so–called "principal whisker" was then chosen for the recording, and the evoked LFPs are recorded from all the cortical layers with a 90 μm recording pitch. For each depth, 100 single LFPs with 500 ms duration were recorded at 20 kHz sampling rate. An open source software, 'WinWCP' (Version: 4.1.0) developed by the SIPBS, University of Strathclyde, UK (http://spider.science.strath.ac.uk/sipbs/software_ses.htm) was used for recording the signals.

3. Results and discussion

The method was implemented in MATLAB (Version: 7.9, release: 2009b, website: http://www.mathworks.com). As the method was designed keeping in mind all kinds of users (with or without programming experience), an easy to use Graphical User Interface (GUI) was also included to encapsulate the coding for the non–programming background users. The GUI is shown in figure 3.

To check the method's workability it was applied on a number of datasets and the results were found satisfactory except some exceptional cases, when the signal morphology was completely different from that of the barrel cortex. As seen in figure 1, each depth profile or

dataset recorded from an experiment comprised of recordings from about 20 different cortical positions, and each of them contained as many as 100 single sweep LFPs. In addition, to demonstrate the distribution of single LFPs in different clusters, we also present clustering results related to a representative set of single LFPs. However, the usefulness of this method is evidenced through experimental findings.

In figure 4 we can see the raw single LFPs and their average signal (left) and the estimated single LFPs and their average signal (right). The arrow indicates the stimulus–onset which is the starting point of the template. The main reasons behind performing the estimation are two folds. Firstly, reduction of noise and oscillations without filtering out vital signal information; secondly, as the single sweep signals contain heavy oscillations, the signal characteristics (E1–E4) are often hidden. Thus, the smoothing facilitates the recognition of these events to be used as the basis for generating the feature vector for the *i*K–means clustering.

After generation of the template, each single sweep signals were truncated to the size of the template. This was done to facilitate the recognition process as each single sweep signal was checked for their conformity within the specified bounding conditions. The figure 5 shows the single LFPs truncated and zero–padded to the size of the template (in blue), the upper and lower bounds of the template (in green), and the template itself (in red). We can also see the recognized signals which were within the upper and lower bounds. The classification method provided two means to perform the signal recognition: Contour Matching, and Matched Filter. The method was applied on a dataset using both the methods. When compared, the results of the single sweep recognition varied for both the methods as reported in figure 6. In case of the signals recorded from the upper cortical layers (layer I and II) the matched filter could recognize more signals, but

in general the contour matching method provided a better signal recognition considering all the recording positions.

The *N* recognized single LFPs, each represented by 200 feature points, generate a feature matrix of size $200 \times N$. The features of each single sweep were selected based on the detected events (E1–E4, see Section 1, paragraph 4) in combination with the stimulus–onset and the end of response. Within the range of these six points 194 more points were selected. To retain more information regarding the signal shape, relatively more points were selected near the events' peaks than in distant locations (in a range of ±5 ms from each event's peak one point every 250 µs was selected). Furthermore, clustering with a feature matrix of size $400 \times N$ was also done and not much difference in terms of signal classification was noticed. This feature matrix was then classified using the *i*K–means clustering and the result on a representative dataset is shown in figure 7. In the figure we can see that the single LFPs were classified as per their shape into seven different clusters, also, the averages (in red) of each cluster contained significant shape difference.

To check the automatic and intelligent assignment of the total cluster number by the method, we tabulated in Table I the recording depths, total number of recognized signals, and single sweep distribution among different clusters. This table shows that the feature matrix was well classified into different clusters using the *i*K–means clustering.

Once the single sweep clusters were formed, the program computed local averages of each cluster for further processing. Analyses of these local averages (e.g., event latency, and amplitude calculation) have revealed that the underlying neuronal network generating the signal may be different even if we are recording signals from the same recording site under the same

313 stimulus. Figures 8 and 9 show different latencies and amplitude differences calculated from the
314 various clusters' local averages. These differences in latencies and amplitudes clearly specify the
315 shape variations of among the local averages.

316 Also, the latencies and amplitudes of E2 in each recognized and clustered single LFPs
317 were calculated. The mean latencies and amplitudes of the E2 among different clusters showed
318 variations as seen in figure 10. The variations may as well indicate that the signals were recorded
319 from neuronal populations of different distance from the recording electrode. As the position of
320 the recording electrode was fixed, we may conclude that the signals were generated by activation
321 of different neuronal networks close to the recording electrode.

322 Basing on these evidences, we can assert that the automated method can cluster the single
323 sweep LFPs successfully basing on their different shapes. The results on the latency and
324 amplitude of local averages and individual clusters demonstrate the reliability and usefulness of
325 the method.

326 **4. Conclusions**

327 Through whisking rats perform very fine discrimination of the environment. To better
328 understand the tactile information processing pathway, scientists frequently rely on LFPs as their
329 shapes work as 'fingerprints' of the neural network activities near the recording electrode. To
330 assess multiple networks' activity at one position, it is necessary to distinguish between the
331 different shapes of signals recorded at a single recording site. Till date scientists have relied on
332 single conventional average. Based on previous work and on results presented in this paper, it
333 can be seen that under the same stimulation condition different signal processing pathways can
334 get activated within the neuronal networks close to the recording electrode. Our automated

335 detection method will therefore facilitate the dissection of real network activity from averaged
336 responses. This module is a part of the SigMate software package, which will soon be made
337 available to the research community [15].
338

339 **ACKNOWLEDGMENTS**

340 This work was carried out as a part of the European Commission funded CyberRat project under
341 the Seventh Framework Programme (ICT-2007.8.3 Bio-ICT convergence, 216528, CyberRat).
342

343 **REFERENCES**

344 [1] M. Maschietto, M. Mahmud, S. Girardi and S. Vassanelli, "A high resolution bi–directional
345 communication through a brain–chip interface," *Proc. of 2009 ECSIS Symp. on Advanced*
346 *Technologies for Enhanced Quality of Life (AT–EQUAL 2009)*, 1: 32-35, 2009.
347 [2] A. Legatt, J. Arezzo and H. G. Vaughan, "Averaged multiple unit activity as an estimate of
348 phasic changes in local neuronal activity: effects of volume-conducted potentials," *J.*
349 *Neurosci. Methods*, 2(2): 203-217, 1980.
350 [3] J. van Hemmen and R. Ritz, "Neural coding: A theoretical vista of mechanisms, techniques,
351 and applications," in: *Lecture Notes in Computer Science, Analysis of Dynamical and*
352 *Cognitive Systems*, S. I. Andersson (Ed.), Berlin: Springer, 75-119, 1995.
353 [4] M. Okun, A. Naim and I. Lampl, "The subthreshold relation between cortical local field
354 potential and neuronal firing unveiled by intracellular recordings in awake rats," *J. Neurosci.*,
355 30(12): 4440-4448, 2010.
356 [5] R. Q. Quiroga, "Spike sorting," *Scholarpedia*, 2(12): 3583, 2007. Available:
357 http://www.scholarpedia.org/article/Spike_sorting
358 [6] K.F. Ahrens and D. Kleinfeld, "Current flow in vibrissa motor cortex can phase–lock with
359 exploratory rhythmic whisking in rat," *J. Neurophysiol.*, 92: 1700-1707, 2004.
360 [7] E. Kublik, "Contextual impact on sensory processing at the barrel cortex of awake rat," *Acta.*
361 *Neurobiol. Exp.*, 64: 229-238, 2004.
362 [8] M. Mahmud, A. Bertoldo, M. Maschietto, S. Girardi and S. Vassanelli, "An automated
363 method for detection of layer activation order in information processing pathway of rat
364 barrel cortex under mechanical whisker stimulation," *J. Neurosci. Methods*, 196(1): 141-150,
365 2011.

[9] M. Mahmud, D. Travalin, A. Bertoldo, S. Girardi, M. Maschietto, and S. Vassanelli, "An automated method for clustering single sweep local field potentials recorded from rat barrel cortex," *Proc. ISSNIP Biosignals and Biorobotics Conf. 2011*, 1: 1-5, 2011.

[10] K. Madsen and H. B. Nielsen and O. Tingleff, *Methods for Non–Linear Least Squares Problems (2nd ed.)*, Kgs. Lyngby: Informatics and Mathematical Modelling, Technical University of Denmark (DTU), 2004.

[11] J. Macqueen, "Some methods for classification and analysis of multivariate observations," *Proc. Fifth Berkeley Symp. on Math. Statist. and Prob.*, 1: 281-297, 1967.

[12] H. H. Bock, "Clustering methods: a history of K–Means algorithms," in: *Selected contributions in data analysis and classification*, P.D. Brito, G. Cucumel, F. de Carvalho (Eds.), Heidelberg: Springer Verlag, 161-172, 2007.

[13] M. M. T. Chiang and B. Mirkin, "Intelligent choice of the number of clusters in K-means clustering: an experimental study with different cluster spreads," *J. Classif.*, 27(1): 3-40, 2010.

[14] L.W. Swanson, *Brain Maps: Structure of the Rat Brain*, London: Academic Press, 2003.

[15] M. Mahmud, A. Bertoldo, M. Maschietto, S. Girardi and S. Vassanelli, "SigMate: A MATLAB–based neuronal signal processing tool," *Conf. Proc. IEEE Eng. Med. Biol. Soc.*, 1: 1352-1355, 2010.

FIGURE CAPTIONS

Figure 1: Depth profile of LFPs recorded from the E1 barrel column by stimulating the E1 whisker where the different features of the signals can be easily seen. Each LFP shown here is average of 100 single signals.

Figure 2: Signal acquisition setup showing its different components (top). The stimulus is shown at the bottom which is used in driving the speaker.

Figure 3: The GUI of the LFP sorting method with its components. The plotted 100 single sweep LFPs of a recording session give an idea about the varied shapes that may be present in recordings.

Figure 4: Single LFPs: on left, raw LFPs without smoothing or estimation with average (in red) and on right, estimated LFPs with average (in red). The arrow shows the stimulus–onset i.e., the starting point of the template. The noise in the raw single LFPs is evident in the left figure.

Figure 5: The template (in red), the upper and lower bounds (in green), and the single LFPs truncated to the size of the template (in blue). Also the recognized single signals whose data points fall within the bounds can be seen.

Figure 6: Comparison of single sweep matching using contour matching method and matched filter method.

Figure 7: Clustering result using *i*K–means clustering method. Single LFPs (in blue) and their respective averages (in red) depict clear differences in the shapes among signals of different clusters.

Figure 8: Latency variation among different clusters local averages. Each bar corresponds to a local average of a cluster and each color corresponds to a recording depth consisting of a number of clusters.

Figure 9: Amplitude variation among different clusters local averages.

Figure 10: Cluster-wise mean latency (top) and mean amplitude (bottom) of signals recorded from 720 µm. The error bars indicate the standard deviation.

TABLE CAPTIONS

Table I: Total recognized single LFPs, and single sweep allocation to different clusters. "--" denotes no clusters.

Figures:

Figure 1

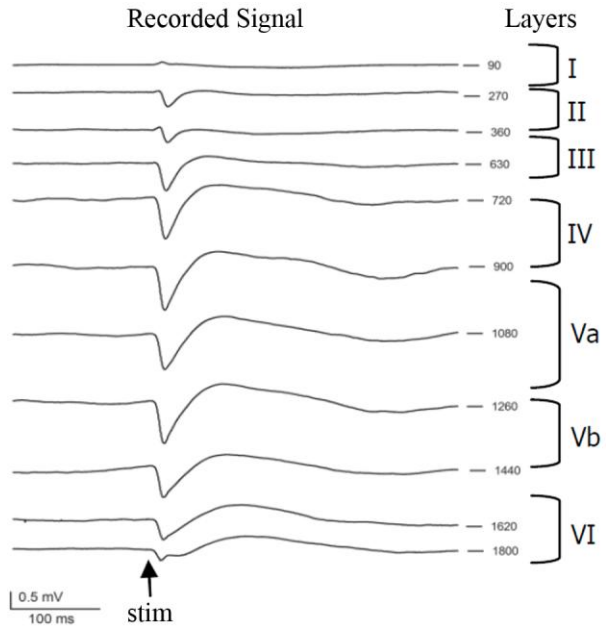

Figure 2

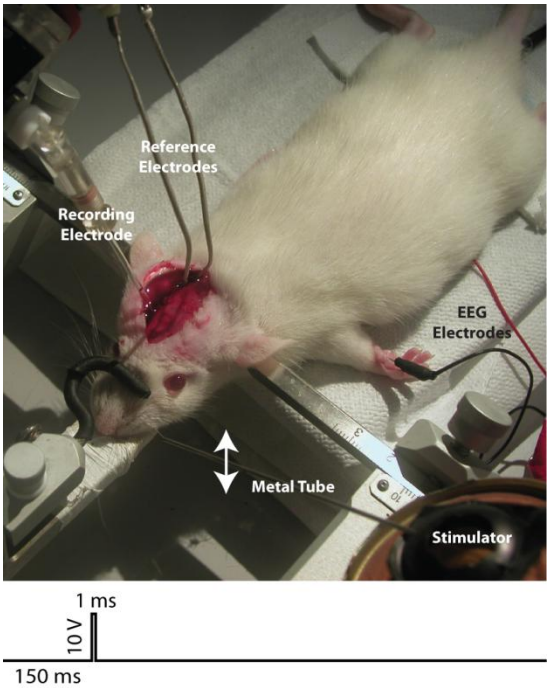

Figure 3

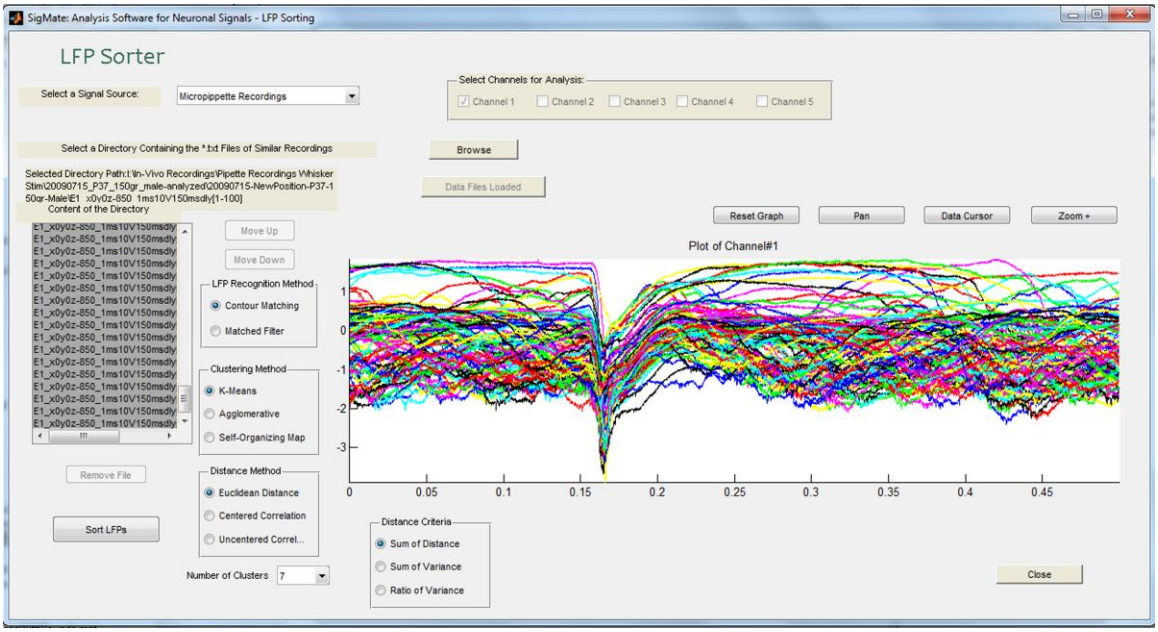

Figure 4

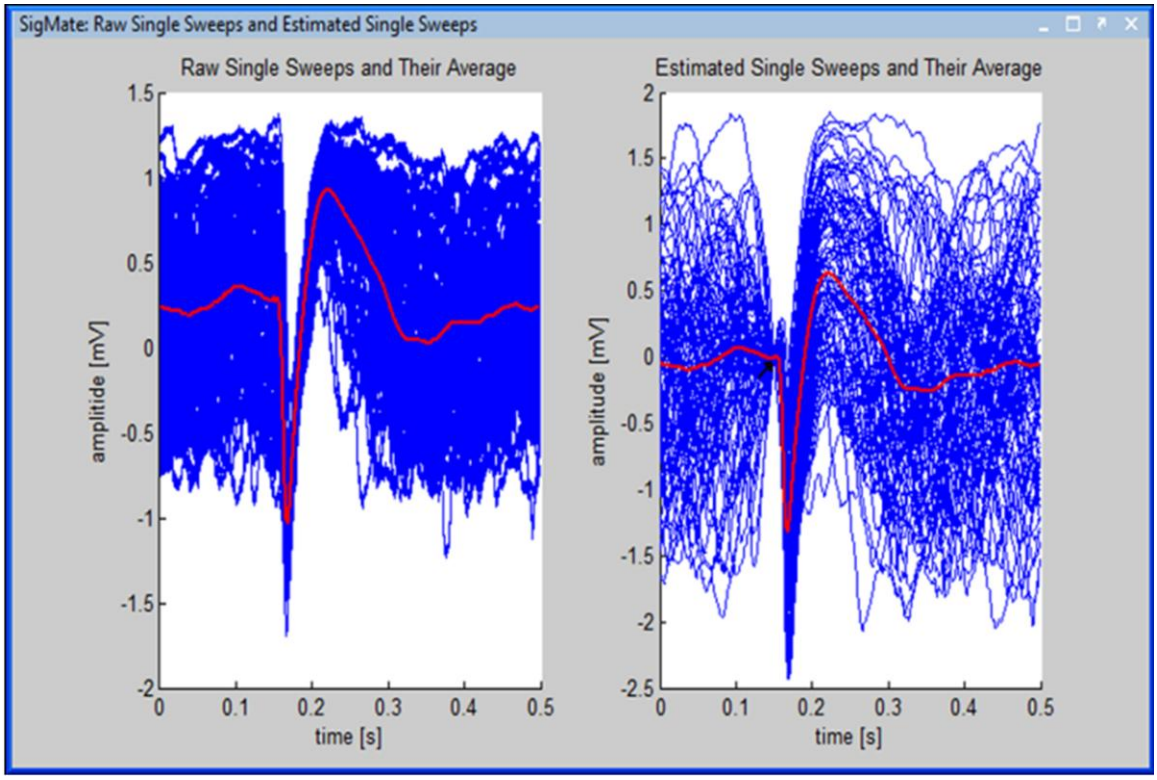

Figure 5

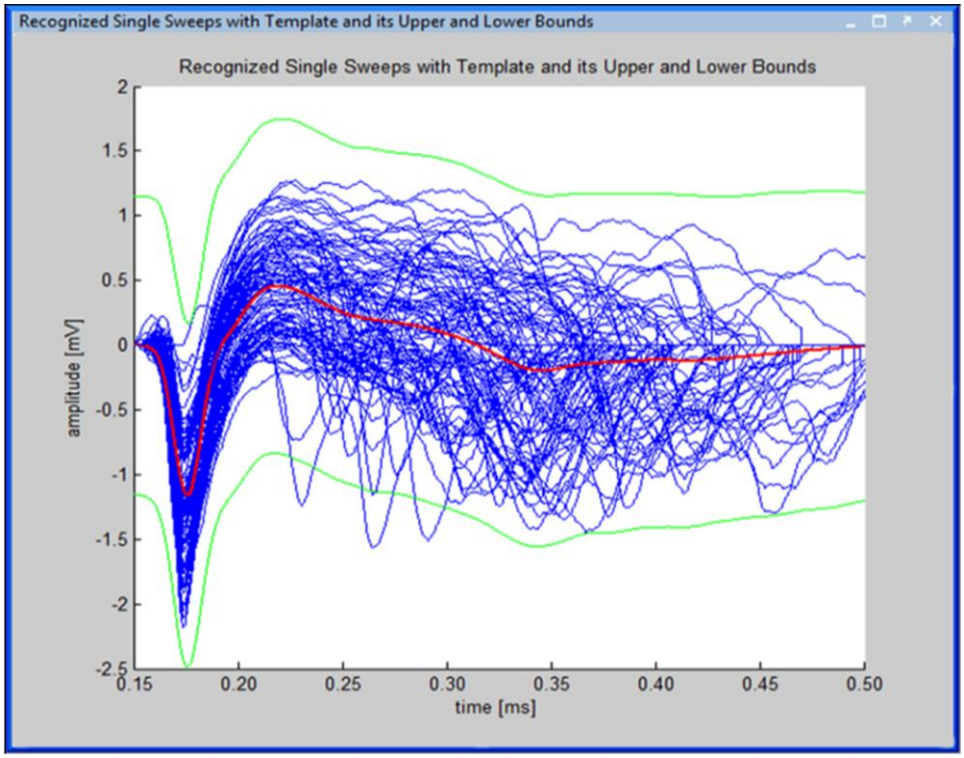

Figure 6

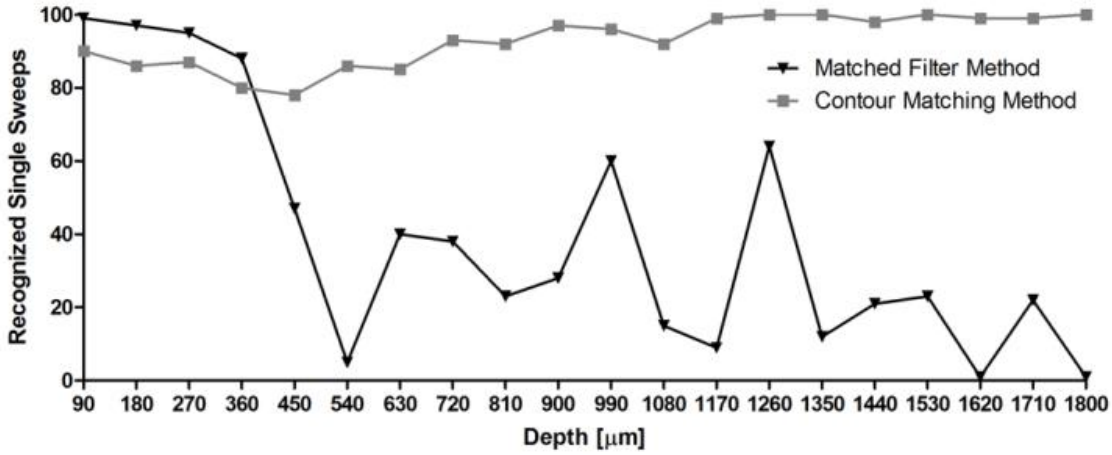

Figure 7

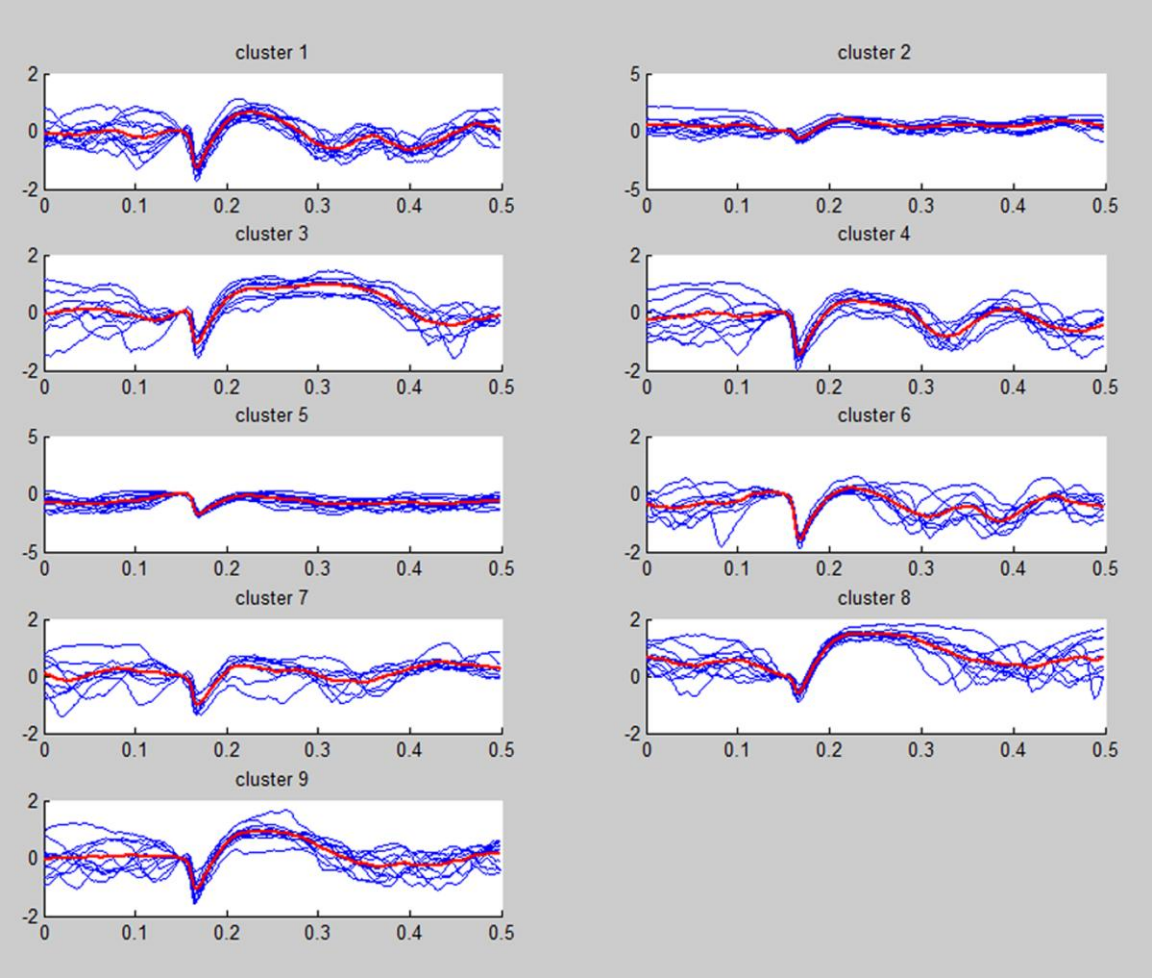

Figure 8

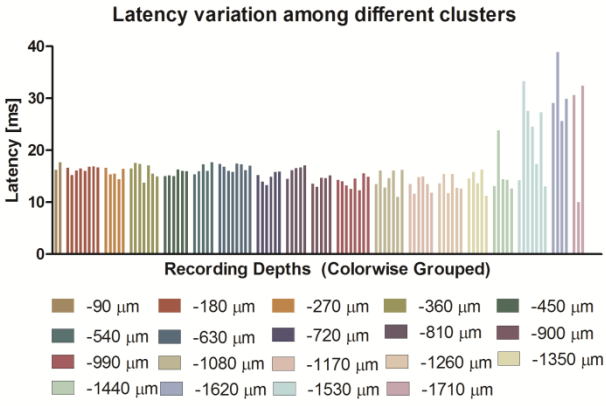

Figure 9

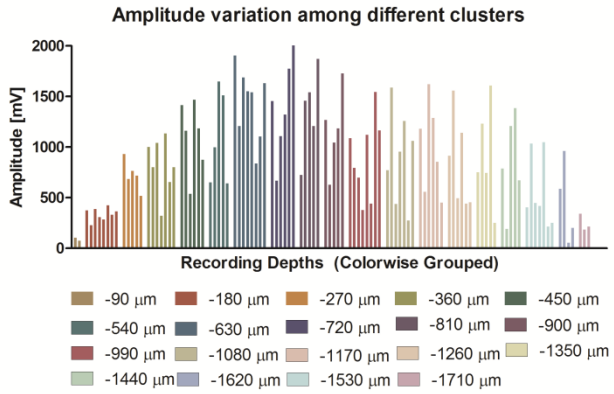

Figure 10

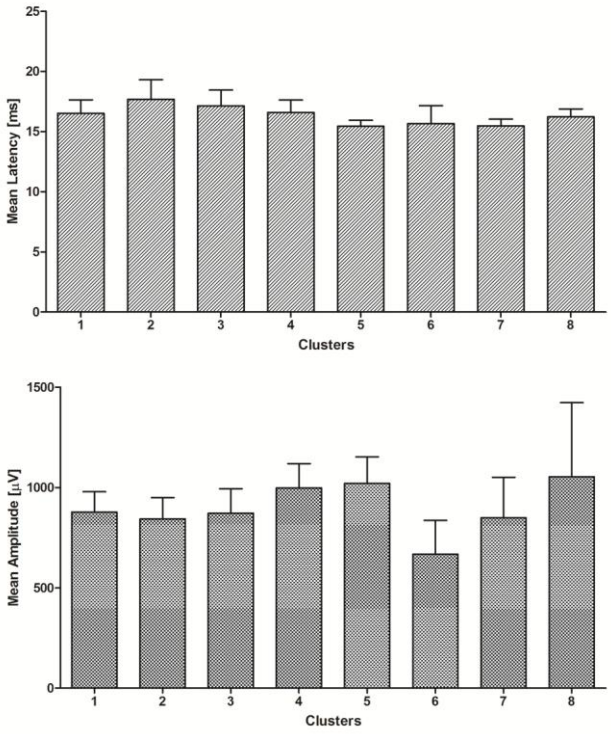

Tables:

Table I

Recording Depth [µm]	Recognized Single LFPs	Clusters Numbers									
		1	**2**	**3**	**4**	**5**	**6**	**7**	**8**	**9**	**10**
90	90	5	6	12	11	11	7	8	12	6	12
180	86	11	17	10	17	18	13	--	--	--	--
270	87	8	8	8	11	15	7	4	10	10	6
360	80	7	10	7	10	13	9	11	9	--	--
450	78	10	9	11	4	7	15	9	13	--	--
540	86	9	8	16	9	9	2	9	8	7	9
630	85	16	6	15	14	17	17	--	--	--	--
720	93	6	18	17	16	7	16	13	--	--	--
810	92	10	9	13	9	13	8	14	6	10	--
900	97	11	15	6	8	14	10	6	9	9	9
990	96	19	15	15	10	5	17	15	--	--	--
1080	92	12	12	9	9	12	9	8	10	11	--
1170	99	8	13	13	9	6	11	10	9	10	10
1260	100	11	20	13	16	7	7	16	10	--	--
1350	100	18	13	19	19	19	12	--	--	--	--
1440	98	13	10	16	8	16	14	7	5	9	--
1530	100	7	9	18	7	14	7	10	16	12	--
1620	99	10	5	16	10	11	8	10	12	11	6
1710	99	10	12	20	13	14	12	18	--	--	--
1800	100	10	12	5	15	16	14	9	19	--	--